The decomposition and emission factors of a wide range of PFAS in diverse, contaminated organic waste fractions undergoing dry pyrolysis

Erlend Sørmo[1,2], Gabriela Castro[3], Michel Hubert[143], Viktória Licul-Kucera[5,6], Marjorie Quintanilla[3], Alexandros G. Asimakopoulos[3], Gerard Cornelissen[1,2], Hans Peter H. Arp[1,3]*

1) Geotechnics and Environment, Norwegian Geotechnical Institute (NGI), Oslo, Norway

2) Faculty of Environmental Sciences and Natural Resource Management, Norwegian University of Life Sciences (NMBU), Ås, Norway

3) Department of Chemistry, Norwegian University of Science and Technology (NTNU), NO-7491, Trondheim, Norway

4) Faculty of Engineering, Norwegian University of Science and Technology (NTNU), NO-7491, Trondheim, Norway

5) Institute for Analytical Research, Hochschulen Fresenius gem. Trägesellschaft mbH, Idstein, Germany.

6) Institute for Biodiversity and Ecosystem Dynamics, University of Amsterdam, Amsterdam, Netherlands

*Corresponding author contact details: erlend.sormo@ngi.no

Keywords

Pyrolysis, sewage sludge, organic waste, PFAS, biochar, method development, emission factors, mass balance

Highlights

- A robust protocol for determination of PFAS in complex matrices such as sewage sludge and biochar.
- Multiple PFAS congeners present at elevated concentrations in eight different organic waste fractions.
- >95% of PFAS in organic wastes decomposed during dry pyrolysis at temperatures >500ºC.
- Emission factors of PFAS during pyrolysis reported for the first time.
- Emissions dominated by short chain PFAS.

Environmental implications

Dry pyrolysis has been suggested as a promising alternative for handling organic waste as it combines thermal destruction of contaminants, energy generation, and production of useful carbon-rich biochar for diverse applications. Such applications include soil quality improvement or soil amendment for contaminant risk abatement. There are, however, uncertainties related to the fate of organic contaminants in the pyrolysis process. The present study presents the decomposition and emission factors of a wide range of PFAS during the dry pyrolysis of diverse organic wastes, thus providing important information for future assessments on the environmental impact of pyrolysis as a waste handling option.

48 Graphical Abstract

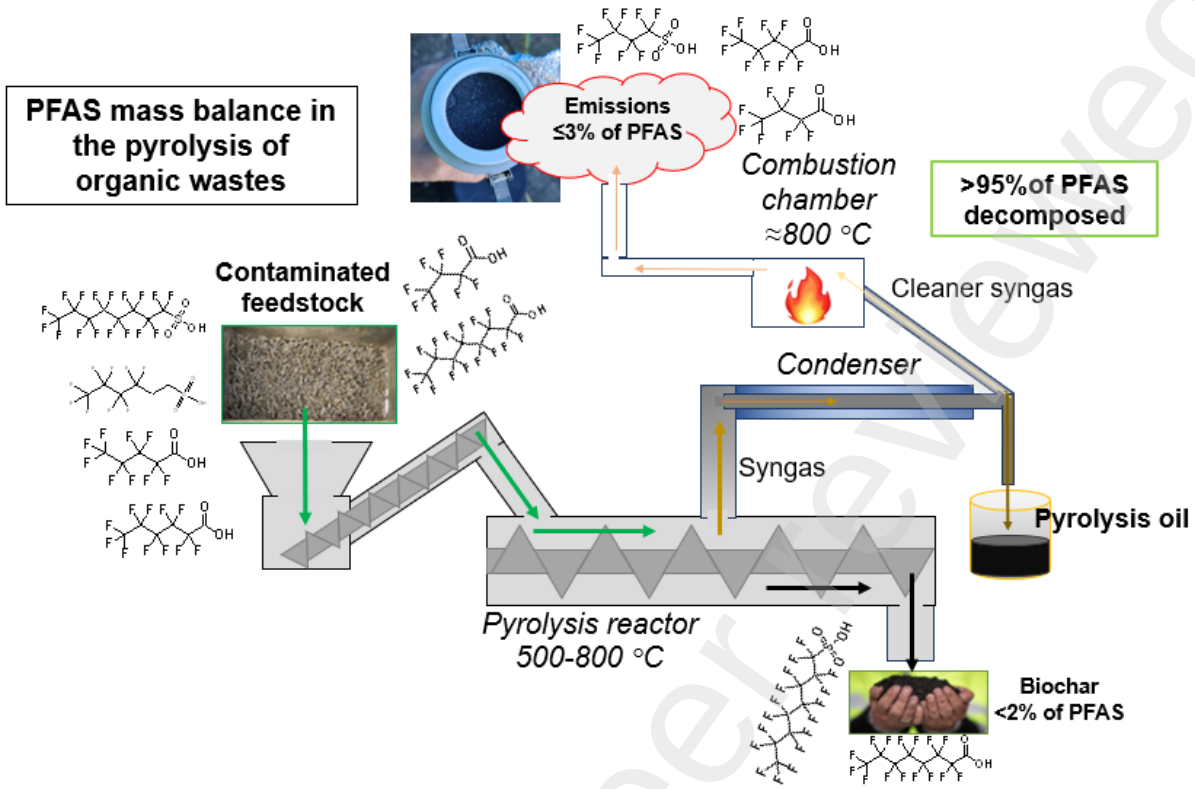

49

50

51 Abstract

52 Current treatment options for organic waste contaminated with per- and polyfluoroalkyl substances
53 (PFAS) are generally limited to incineration, composting or landfilling, all resulting in emissions. Dry
54 pyrolysis is a promising emerging waste handling alternative for contaminated organic wastes,
55 recycling them to biochar, condensate and syngas products for various purposes. However, there is
56 uncertainty related to the fate of organic contaminants like PFAS during dry pyrolysis. The present
57 work first developed a robust method for the determination of PFAS in complex matrices, such as
58 sewage sludge and biochar. Then, a mass balance was established for 56 different PFAS during the
59 medium-scale pyrolysis (500-800 °C) of sewage sludges, food waste reject, garden waste and waste
60 timber. PFAS were found in all wastes (56 to 3651 ng g^{-1}), but pyrolysis resulted in a ≥98% removal.
61 Residual PFAS (0.1-3.4 ng g^{-1}) were detected in biochars obtained at temperatures up to 750 °C.
62 Emitted PFAS loads ranged from 0.01 to 3.1 mg $tonne^{-1}$ of biochar produced and were dominated by
63 short chain PFAS. Emissions made up <3% of total PFAS-mass in the wastes. Remaining

uncertainties are mainly related to the presence of thermal degradation products in flue gas and condensation oils.

1. Introduction

Per- and polyfluoroalkyl substances (PFAS) are a large group of synthetic organic chemicals used in an ever-widening range of industrial and consumer applications since the 1940s (Glüge et al., 2020). Their spreading in the environment has led to adverse health effects, particularly endocrine disruption and carcinogenicity (Sunderland et al., 2019). The strong carbon-fluorine bonds confer them high thermal stability, persistence and relatively high water solubility, which have made them ubiquitous in the environment (Abunada, 2020; Krafft & Riess, 2015). Particularly, compounds such as perfluoroalkyloctanoic acid (PFOA) and perfluoroalkyloctanoic sulfonate (PFOS) have been included in the Stockholm Convention (UNEP, 2017, 2019), and thus, their production has shifted from long chain ($CF_2 \geq 7$, where CF_2 represents the number of perfluorinated alkyls in a chain) towards short chain ($6 \leq CF_2 \geq 4$) and ultrashort chain ($3 \leq CF_2 \geq 1$) PFAS compounds (Ateia et al., 2019; Buck et al., 2011). The high mobility of short chain and ultrashort chain PFAS makes them spread fast in the environment and challenging to remove, e.g., in wastewater treatment plants (WWTPs), leading to a widespread occurrence in drink water sources (Neuwald et al., 2022). Lately, attention has also been given to PFAS precursor compounds, such as perfluorooctylsulfonamides (FSA) and fluorotelomer alcohols, due to both the discovery of their toxicity and their environmental transformation pathways (Zhang et al., 2021).

Due to their widespread use and environmental presence, PFAS compounds find their way into most waste streams, including municipal solid waste (Allred et al., 2015), electronic waste (Tansel, 2022), sewage sludge (Gallen et al., 2018; Venkatesan & Halden, 2013), animal manure (Munoz et al., 2022) food waste (O'Connor et al., 2022), composite wood building materials and textile waste (Bečanová et al., 2016). Inadequate treatment of such waste streams has led to PFAS compounds being spread in the environment (Lang et al., 2017; Sepulvado et al., 2011), and also presents a major challenge for recycling in the circular economy (Hale et al., 2022).

Modern waste incineration, usually operated at >1000 ºC, has been an accepted approach to handling hazardous waste in many regions (Block et al., 2015; Dempsey & Oppelt, 1993), as modern waste incinerators readily degrade most organic contaminants and are designed with flue gas scrubbing and energy recovery. The fate of PFAS during waste incineration processes is not well understood and there are both concerns about unmonitored compounds, such as precursors, and ultrashort chain PFAS, and environmental risks related to the release of thermal degradation products (Stoiber et al., 2020). During the last decades, pyrolysis has received increased attention from the scientific community as a more sustainable thermal handling option for organic waste (Beesley et al., 2011; Lehmann et al., 2006; Li et al., 2019; Xiao et al., 2018). Pyrolysis entails heating up organic waste in absence of oxygen to produce syngas, oil and biochar (Barry et al., 2019). Biochar is a porous carbon-rich product, with a versatile set of characteristics that can be exploited for multiple usages, such as agricultural soil improvement (Hale et al., 2020; Ippolito et al., 2015; Obia et al., 2016) carbon capture and storage (Schmidt et al., 2019), sorbents for organic contaminants (Ahmad et al., 2014; Alhashimi & Aktas, 2017; Hale et al., 2016) fillers in concrete (Gupta & Kua, 2019), and substitutes for anthracite coal in metallurgical industry (Ye et al., 2019). Furthermore, the effect of pyrolysis as a thermal treatment option to decompose organic contaminants has been demonstrated for pharmaceuticals, polychlorinated biphenyls (PCBs), polyaromatic hydrocarbons (PAHs) and endocrine disrupting and hormonal compounds (Moško et al., 2021), chlorophenols and chlorinated pesticides (Sørmo et al., 2020), as well as organophosphorus flame retardants (Castro et al., submitted).

Recently, Alinezhad et al. (2022) demonstrated for soils that the type of thermal treatment, incineration or pyrolysis, does not matter in terms of PFAS removal as long as temperature and residence time are sufficient, i.e. >500 °C and >30 min, respectively. Other laboratory studies (Xiao et al., 2020; Yao et al., 2022) have documented the degradation of a wide range of PFAS compounds, in spent activated carbon (AC) or in aqueous film forming foam (AFFF) respectively, under an inert atmosphere and similar conditions, and were able to detect a range of perfluoroalkene-, perfluoroalkane-, perfluoroalkyl aldehyde- and fluorotelomer alcohol degradation products. Nonetheless, they were not able to detect the specific ozone-harming perfluoroalkanes,

perfluoromethane and perfluoroethane, or other short chain polyfluoroalkane greenhouse gases. These results are promising for pyrolysis as a waste handling alternative for PFAS-contaminated organic waste. However, as Stoiber et al. (2020) noted in the case of waste incineration, the effects demonstrated in idealized laboratory studies might not be the same for full scale operations. Such a discrepancy has previously been documented in data from sewage sludge pyrolysis in two commercially operated plants that show the presence of PFAS in flue gas scrubber water (Thoma et al., 2022), although at low concentrations (PFOA at 13.2 ng L^{-1} and PFOSA at 46.2 ng L^{-1}). This suggest that PFAS compounds to some extent can survive a sequence of high temperature pyrolysis and combustion in an upscaled system.

Hence, the purpose of the present study was to fill knowledge gaps related to the fate of PFAS during real-world, industrial pyrolysis of contaminated organic waste by exploring how feedstock and pyrolysis conditions affect the presence of PFAS in both biochar and the emitted exhaust from a medium scale pyrolysis system (operational up to 5-10 kg hr^{-1}). This was performed by testing the following hypotheses: 1) Given a high enough pyrolysis temperature, PFAS will be removed from the solid phase (feedstock to biochar) regardless of initial concentrations and composition of congeners and 2) a pyrolysis mass balance that includes emission factors will demonstrate that the majority of quantifiable PFAS compounds are decomposed in the process. This study presents the first investigation of PFAS in pyrolysis of organic waste types other than sewage sludge. To the best of the authors' knowledge, it is also the first to quantify the potential release of PFAS compounds from a medium scale pyrolysis system, let alone provided emission factors for PFAS from pyrolysis. This study also considered 56 different compounds, including ultrashort chain PFAS and PFAS precursors, which required the development of a novel and robust method for PFAS analysis in complex matrices such as sewage sludge and biochar.

2. Materials and methods

2.1 Chemicals and materials

PFAS standards were acquired from various providers or self-synthesized (see Table S1 for full details). Isotopically labelled internal standards: PFOA-$^{13}C_8$ (99%), PFOS-$^{13}C_8$ (99%) and 6:2 FTS-$^{13}C_2$-D_4 were bought from Cambridge Isotope Laboratories.

LC-MS grade Methanol (MeOH) and acetonitrile (CAN) was purchased from Merck (Darmstadt, Germany). Ethyl acetate (EtOAc, ≥99.7% v/v), ammonium acetate (≥98% w/w) and formic acid (FA, 96%) were supplied by VWR Chemicals (Trondheim, Norway). Ammonium acetate (>99% w/w) was bought from Fluka (Munich, Germany). Water was purified with a Milli-Q grade water system (Q-option, Elga Labwater, Veolia Water Systems LTD, U.K.) or purchased (LiChrosol®, UHPLC-MS grade) from Merck (Darmstadt, Germany). Whatman® Glass fiber filters (GFF) and Amberlite® XAD-2® was purchased from Merck (Darmstadt, Germany). Nitrogen (N_2, ≥99.6%) was acquired from Linde Gas AS (Oslo, Norway).

2.2 Contaminated organic waste fractions

Waste fraction descriptions

Seven contaminated waste materials, and one reference material, were investigated in this study (Table 1). The waste materials included four sludges from wastewater treatment plants, one reject from food waste biogas production, and three wood-based fractions – waste timber, garden waste and wood chip pellets from forestry/logging. Based on existing literature, the waste fractions investigated were all expected to contain different concentrations of PFAS. The raw waste samples will be referred to as feedstocks for the pyrolysis process for the remainder of this study.

Bulk sampling and pre-treatment before pyrolysis

Samples of about 2 m^3 were collected in bulk at a randomly chosen time point for each feedstock by the respective waste handling companies/wastewater treatment plants. The full-size bulk samples

were dried (moisture content 5-10%) using a batch paddle drier (1.5 x 5 m) made by Scanship AS (Tønsberg, Norway). The drier heats the sample material to about 102-110 °C by channelling superheated steam from a heat exchanger into a heating jacket fitted around the drier. The dried feedstocks were then pelletised (length 40 mm, radius 8 mm). Both pre-treatments, drying and pelletisation, were applied to homogenize the chemical composition and physical properties of the feedstocks before pyrolysis.

Table 1. Description of the waste material feedstocks studied, conditions for their respective pyrolysis treatments, and sampling information.

Feedstock	Abbrev.	Description	Pyrolysis temperatures (ºC)	Pyrolysis residence time (min)	Solid phases sampled	Flue gas sampled
Digested sewage sludge	DSS-1	Sewage sludge and food waste gone through thermal hydrolysis (170 ºC) before anaerobic digestion for biogas production	500, 600, 700 and 750	20	Yes	Yes (excl. 750 ºC)
Digested sewage sludge	DSS-2	Sewage sludge gone through anaerobic digestion for biogas production	500, 600, 700 and 800	20	Yes	Yes
Limed sewage sludge	LSS	Sewage sludge gone through anaerobic digestion for biogas production, then added lime (39%) for stabilization/hygenization	600 and 750	20	Yes	Yes
Dewatered sewage sludge	DWSS	Raw sewage sludge, thermally hydrolysed (170 °C) and then dewatered using a heated centrifuge (100 °C).	600, 700 and 800	40	Yes	No
Reject from food waste biogas production	FWR	Fraction of food waste rejected from biogas production. Consists of material that does not pass an initial sieving process to reject plastics and other too large or non-digestible items.	600 and 800	20	Yes	No
Waste timber	WT	Discarded wood products and objects from private households, businesses and construction/demolition (no chemically impregnated wood)	500, 600, 700 and 800	20	Yes	No
Garden waste	GW	Gardening waste from private households and businesses. Fraction includes twigs, leaves, roots and some sand/gravel.	500, 600 and 800	20	Yes	No
Wood chips	CWC	Pellets produced from pine wood chips from forestry/logging.	500, 600, 700 and 750	20	Yes	No

2.3 Pyrolysis

Pyrolysis technology

A medium scale Biogreen® pyrolysis unit (2-10 kg biochar/hr) built by ETIA Ecotechnologies (now a part of VOW ASA, Lysaker) was used in the present study (Figure S.1). In this unit, feedstock material was fed through a feeding screw with a vacuum lock, into the pyrolysis reactor which

contains an electrically heated screw, the Spirajoule©, with a maximum temperature of 900 ºC. The feedstock material was converted to biochar as it moved along the screw, and residence time in the reactor was controlled by the rotational frequency of the screw. The reactor was run on a negative pressure to allow pyrolysis gas to be quickly separated from the biochar, as to minimize contact time between biochar and gas. The pyrolysis gas was channelled directly into a condenser unit where the gas was cooled to approximately 10 ºC. Pyrolysis oil was collected through a liquid lock while the syngas continued into a burner where it was combusted with propane at 800-900 ºC before being released as exhaust through a chimney.

Operational conditions

Feedstock feeding rates of 5-10 kg hr^{-1} were used. The wood-based substrates (wood chips, waste timber and garden waste) were run at around 5 kg hr^{-1}, to avoid tar-clogging between reactor and the condenser, while some of the sludge-based materials were run at rates closer to 10 kg hr^{-1}. To remove O_2 from the system, the reactor and connecting pipes were flushed with N_2 for 10 min before the start. Residence time in the reactor was 20 min for all samples except the de-watered sewage sludge, for which a 40 min residence time was used. The change in residence time for this feedstock only, was the result of a need to address technical challenges related to clogging of the feeder screw.

Pyrolysis temperature was considered the main treatment variable in this study, and the samples were pyrolyzed at two or more temperatures between 500 and 800 ºC (see Table 1 for details). Not all feedstocks were pyrolyzed at the same set of temperatures due to a combination of logistical and technical challenges. Treatment temperature was defined as measured in the biochar leaving the reactor at the end of the heated screw. After the pyrolysis set point temperature was reached, the reactor was run for another 1-2 hours in order to reach stable conditions before sampling.

Gas emission measurements and sampling of biochar were done only during the period of stable conditions, which lasted approximately 2 hours for each treatment temperature.

Biochar yield ($Y_{Biochar}$, %) at a specific treatment temperature was determined as the rate of biochar produced ($R_{biochar}$, kg hr^{-1}) divided by the feedstock feeding rate ($R_{feedstock}$, kg hr^{-1}) over the period defined as stable conditions:

213 $$Y_{Biochar}\,(\%) = \frac{R_{Biochar}\,(kg\ hr^{-1})}{R_{Feedstock}\,(kg\ hr^{-1})} \times 100 \qquad \text{(Eq. 1)}$$

214 As a control, yield was also calculated for each step in the pyrolysis process (heating, stabilization and
215 cooling), and the sum of these respective yields were compared to the yield calculated by total
216 feedstock in and total biochar out for the entire pyrolysis run.
217

218 ## 2.4 Sampling and emission measurements

219 Solids sampling

220 Feedstock subsamples for chemical characterization were taken by random grab sampling (10-20
221 scoops, 1 kg) during the pelletisation process. Biochar subsamples were composed by random grab
222 sampling (10-20 scoops, 1 kg) from the total amount of biochar (2-10 kg) produced during each
223 treatment temperature. Both feedstock and biochar subsamples were air dried in the laboratory,
224 crushed (D< 1 mm, controlled by sieve) and homogenized using a ball mill (Retsch ISO 9001) at 50
225 rpm for 10 minutes. Between each sample, the ball mill was scrubbed with soap, rinsed twice with
226 MeOH:MiliQ (50%) and dried (100 ºC, 10 min).

227 Pyrolysis oil was collected in bulk through a liquid lock throughout the period of stable
228 conditions. The bulk sample was split into an aqueous and an oil phase using a phase separating
229 funnel. The fractions were weighed to establish the ratio between oil and water, before subsamples
230 were collected by vigorously shaking and then pouring out the relative amounts of each phase to
231 produce a smaller (100 mL) sample in HDPE bottles.
232

233 Gas Emission sampling

234 Exhaust gas and aerosols were sampled from inside the chimney (the only exit for flue gas), within
235 the inner 2/3 of the chimney diameter at about 20 cm below the outlet. Gas measurements were done
236 for all the sewage sludge-based feedstocks, except for the DWSS (all treatments) and the DSS-1 (750
237 ºC treatment).

Particle based and gas phase contaminants in the exhaust were sampled using a low volume air sampler (Comde-Derenda, Stahnsdorf, Germany), operated at a rate of 2.4 m^3h^{-1}, that draws flue gas from the chimney into a cartridge with a GFF for aerosol collection (0.45 µm, pre-cleaned by heating to 450 °C for 8 hrs) followed by an XAD-2 sorbent for gas phase contaminants (dried at 105 °C for 24 hrs and pre-cleaned through Soxhlet-extraction with MeOH, acetonitrile, toluene (8 hrs per solvent) and cyclohexane 4 hrs, ≈100 mL per sampling). A single point sample integrated over a period of 60 minutes was collected for each treatment temperature. The filter cartridge was rinsed with MeOH between each sampling. The combination of GFF and XAD-2 in a low volume air sampler has previously been used successfully in ambient air sampling of PFAS (Barber et al., 2007).

Carbon based gas composition of the exhaust – carbon monoxide (CO), carbon dioxide (CO_2), methane (CH_4), and non-methane volatile organic carbon [NMVOC = ethane (C_2H_6) + propane (C_3H_8) + ethylene (C_2H_4) + hexane (C_6H_{14}) + formaldehyde (CHOH)], in addition to hydrofluoric acid (HF), was determined using a portable Fourier Transform Infrared Spectrometer (FTIR) from Gasmet. One data point was recorded every three minutes (n≈40 per treatment). Nitrogen (N_2) content in the sample was corrected for by running a N_2 blank before every sampling. Aerosol concentrations (≤10 µm, PM_{10}) were measured separately every 10-20 minutes (n= 6-12) with a pdr-1500 instrument from Thermo Scientific. PM_{10} concentrations were converted to total suspended particles (TSP) using a factor 1.4, as according to Sparrevik et al. (2015). Gas composition data was used to establish a carbon balance for the process (see section 2.7).

2.5 Sample preparation and instrumental analysis

Carbon analysis

Total carbon in the feedstock and biochar samples was analysed in triplicates using the dry combustion method as described by Nelson & Sommers (1982) with IR on a Leco CHN628 instrument. Total carbon in the pyrolysis oil condensates were determined through conversion of all carbon species to CO_2 through combustion with subsequent infrared detection according to method ASTM D5291 by Karlshammerverket Laboratory, Karlshamn, Sweden.

PFAS analysis

For the PFAS analysis two different extraction methods were used (extraction method A and B), and three different instrumental methods (instrumental method A, B and C). Extraction method A was combined with instrumental method A to target 41 congeners (method AA), while extraction method B was combined first with instrumental method B to target 11 congeners (method BB) and then with instrumental method C to target further 4 congeners (BC).

Extraction method A: This approach required method development, see the SI for details (section B). All feedstock, biochar, XAD and GFF samples were extracted for analysis, in triplicate, targeting 41 congeners that included 15 perfluorinatedalkylcarboxylic acids (PFCA), 9 perfluorinatedalkylsulphonic acids (PFSA), 4 fluorotelomere sulphonates (FTS), 8 fluorosulphonamides (FSA), and 5 miscellaneous substitute compounds. See the full list of congeners in the SI (Section A, and Table S1).

The extraction procedure used was based on Asimakopoulos et al. (2014) with minor modifications: 0.1 g of sample was introduced in a 15 mL PP tube and spiked with 10 ng mL^{-1} of a mixture of ISs. Then, 300 µL of 1M ammonium acetate aqueous buffer was added to the sample to favour the salting-out of analogues with high polarity. Ultrasound assisted extraction (UAE) was performed with 3 mL of EtOAc and ultrasonication (45 min, 40 °C) followed by centrifugation (10 min, 4000 rpm). The supernatant was collected and transferred into a clean PP tube. The UAE was repeated another two consecutive times to produce a final volume of ~9 mL (3 x 3mL). Clean-up was carried out by adding 2 mL Milli-Q water to remove the high salt concentration of ammonium acetate and other polar matrix interferences, and the extract was shaken and centrifuged (10 min, 4000 rpm). The obtained extract was concentrated under a gentle nitrogen stream (N_2, 35 ºC) to near dryness, before being reconstituted in MeOH:Milli-Q (1 mL, 50:50).

Instrumental method A: The instrumental method used was based on Trimmel et al. (2021) with minor modifications**.** Target analytes were determined with UPLC-MS/MS with a Xevo TQ-S

triple quadrupole mass spectrometer, equipped with a Z spray ESI source, connected to an Acquity UPLC I-Class system, both acquired from Waters (Milford, MA, U.S.). Analytes were separated using a Kinetex C_{18} column (30 x 2.1 mm, 1.3 µm) serially connected to a C_{18} security guard (2 x 2.1 mm i.d.), both supplied by Phenomenex (Torrance, CA, U.S.). Milli-Q water 2 mM ammonium acetate (A) and MeOH (B), were used as mobile phases at a constant flow rate of 250 µL min^{-1}. The UPLC column and precolumn were maintained at 30 ºC. The mobile phase gradient was programmed as follows: 0-0.2 min, 10% B; 3.0-3.5 min, 100% B; 3.6-5 min, 10% B. The injection volume was 4 µL. Analytes were ionized under negative ionization mode (ESI-), using N_2 as drying gas at the ionization source (450ºC at 650 L $hour^{-1}$). The capillary voltage was maintained at 2 kV, cone voltage at 25 V, and source offset voltage at 40 V. Two transitions were monitored per chemical (Table S2) considering a time window of 60 s around their retention time. The dwell time per transition was automatically adjusted by the MassLynx software to obtain 12 points per peak assuming an average baseline peak width of 5 s.

Extraction method B: Two sewage sludge-based feedstocks (DSS-1 and DSS-2), their resulting biochars and the XAD-resins from gas emission measurements at all treatment temperatures were selected for quantification of additional PFAS. Due to limited sample amounts, GFF samples were not available for these analyses.

The samples were extracted following the protocol suggested by Ahmadireskety et al. (2021) with modifications: 0.2 g of sample was added NH_3/MeOH (1%, 5 mL), before ultrasonication (30 min, 40 °C), followed by centrifugation (10 min, 4000 rpm) and supernatant collection. The procedure was repeated to produce a final supernatant volume of 10 mL, that was reduced under N_2 until near dryness (35 °C), before being reconstituted in MeOH (1 mL). An additional clean up procedure, to minimise matrix interferences, was done by adding the supernatant sample (1 mL) to a mixture of acetic acid (100 µL, anhydrous) and Superclean™ ENVI-Carb™ (50 ± 5 mg). The resulting mixture was shaken vigorously (30 s) and being centrifuged (10 min, 4000 rpm). The supernatant was collected and evaporated under N_2 until near dryness (35 °C), before being reconstituted in acetonitrile:water (95:5) and filtered through a recycled cellulose syringe filter (0.2 µm).

Instrumental method B: This method was used to monitor 11 precursor compounds not included in method A, namely 7 perfluorinated alkanoic acids, 2 perfluoroalkoxy acetic acids and 2 perfluoroalkyl bisphosphates, see the SI for full details (section A, Table S1). They were analysed using reversed-phase liquid chromatography-mass spectrometry (RPLC-MS) on a Nexera XR HPLC system hyphenated to an Sciex QTrap 5500 System. Chromatographic separation was achieved using an XSelect HSS T3 column (50 x 2.1 mm, 3.5 µm) equipped with the corresponding pre-column (5 x 2.1 mm, 3.5 µm) held at 30 °C. The RPLC eluents consisted of water:methanol (95:5, eluent A) and water:methanol (5:95, eluent B) with 5 mM ammonium acetate (5 mM). The gradient started at 0% eluent B, increased to 100% B in 8 min, and held until 12 min. Then the column was re-equilibrated to 0% from 12-12.5 min and held for 6 min. The total run time was 18.5 min, injection volume 10 µL and flow rate was 300 µL min-1.

Instrumental method C: Ultrashort chain PFAS, 4 congeners, including 3 PFCA and 1 PFSA (see SI section A and Table S1) were analysed using hydrophilic interaction chromatography coupled to mass spectrometry (HILIC-MS), as previously described by Neuwald et al. (2022). See the SI (section C) for a detailed description.

Instrumental methods B and C: For the ultrashort chain and additional precursor PFAS in this study no internal standards (or comparable internal standards) were available. Therefore, the actual samples were spiked before extraction and after extraction to evaluate absolute recoveries. The results can be found in Table S4.

2.6. Quality control and assurance

Procedural blanks were analysed to evaluate background contamination arising from the lab materials and solvents. During analysis, solvent blanks, and a standard solution were injected regularly injections to check for any potential cross contamination or sample carryover, and to evaluate signal variations and drift. The injection needle was washed with a solution of MeOH:Milli-Q (50:50; v/v) with 0.1 % FA before and after each injection.

To ensure accuracy and precision, multiple-point calibration curves were prepared: Instrumental method A: 11 points from 0.01 to 50 ng mL^{-1} in MeOH:Milli-Q (50:50, v/v), Instrumental method B: 7 points from 0.05 to 20 ng mL^{-1} in ACN:Milli-Q (95:5, v/v), and Instrumental method C: 7 points from 0.01 to 5 ng mL^{-1} was prepared in ACN:Milli-Q (95:5, v/v), demonstrating regression coefficients for all the studied compounds, R^2>0.98, R^2>0.99 and R^2>0.999, respectively. Two MS/MS transitions were optimized per TA. The most intense transition (higher S/N ratio) was considered as the quantification transition (1) and the second as the confirmation transition (2) (Table S2). The instrumental limits of quantification (iLOQs) were calculated for each target analyte as ten times the signal from the baseline noise (S/N ratio) and ranged from 0.01 to 5.00 ng mL^{-1} (Table S2). The method LOQs (mLOQs) were estimated accordingly with pre-extraction spiked samples and ranged from 0.25 to 50 ng mL^{-1} (Table S2). All samples were analysed in either duplicates (GFF) or triplicates (feedstocks, biochar and XAD) to control for sample heterogeneity and method error. Glass fiber filter samples were analysed in duplicates rather than triplicates due to limited amounts of sample material availability.

Obtained absolute recoveries (Abs%), relative recoveries (Rel%) and matrix effects (ME%) are presented in Table S4. Quantification of the target analytes was accomplished based on the internal standard method and matrix-matched calibration standards (Raposo & Barceló, 2021).

2.7 Data analysis

All concentrations are presented as ng g^{-1} dry weight (d.w.). For statistical analyses the numeric values of 0 and LOQ/2 were used in cases where one or two of the replicate data points were < LOD or LOQ respectively.

To estimate the relative effectiveness of pyrolysis as a waste treatment option for PFAS, the removal efficiency (RE) was calculated according to the equation suggested by Moško et al. (2021):

$$RE\ (\%) = 100\% - \left(\frac{C_{biochar} \times Y_{biochar}}{C_{feedstock}} \right) \qquad \text{(Eq. 2)}$$

where $C_{biochar}$ is the concentration (ng g^{-1}) in a biochar produced at a given pyrolysis temperature, $C_{feedstock}$ is the concentration (ng g^{-1}) in the feedstock and $Y_{biochar}$ is the yield (Eq. 1) of the biochar in the pyrolysis process.

Emission factors in µg $PFAS_{tot}$ per tonne of biochar produced (EF_{PFAS}, µg $tonne_{biochar}^{-1}$) were calculated using the carbon balance approach (Cornelissen et al., 2016; Pennise et al., 2001; Sparrevik et al., 2015; Zhang et al., 2000). This method uses the carbon balance between feedstock going into the process and biochar, pyrolysis oil and flue gas coming out to calculate the net molar component-to-CO_2 emission ratios and is described with an adaptation from Sparrevik et al. (2015) in equations Eq. 3-7.

The mass balance of carbon in pyrolysis of organic waste can be written as:

$$C_{Feedstock} - C_{Biochar} - C_{Pyrolysis\ oil} = C_{CO2} + C_{CO} + C_{CH4} + C_{NMVOC} + C_{TSP} \quad \text{Eq. 3}$$

where $C_{Feedstock}$ is the mass of C in feedstock, $C_{Biochar}$ the mass of C in biochar, $C_{Pyrolysis\ oil}$ the mass of C in pyrolysis oil and C_{CO2}, C_{CO}, C_{CH4}, C_{NMVOC} and C_{TSP} the mass of C in emitted CO_2, CO, CH_4 NMVOC and TSP, respectively. Rearranging Eq. 3 to produce the molar ratio of each component to C_{CO2} gives:

$$\frac{C_{Feedstock} - C_{Biochar} - C_{Pyrolysis\ oil}}{C_{CO2}} = 1 + \frac{C_{CO}}{C_{CO2}} + \frac{C_{CH4}}{C_{CO2}} + \frac{C_{NMVOC}}{C_{CO2}} + \frac{C_{TSP}}{C_{CO2}} = 1 + K \quad \text{Eq. 4}$$

Let the sum of all emitted carbonaceous components then be represented by 1+K. The molar ratios of C in each component (C_{CO}, C_{CH4} etc.) to C_{CO2} is calculated by dividing the ratio of the measured concentrations with the molar mass ratio of said component and CO_2. Now the emission factor of C_{CO2} ($EF_{C\text{-}Co2}$) can be defined as the mass of emitted CO_2 (C_{CO2}) per mass of biochar produced ($m_{biochar}$):

$$EF_{C-CO2} = \frac{C_{CO2}}{m_{biochar}} = \frac{C_{Feedstock} - C_{Biochar} - C_{Pyrolysis\ oil}}{(1+K)m_{biochar}} \quad \text{Eq. 5}$$

$EF_{C\text{-}CO2}$ can subsequently be transformed to represent the emitted mass of CO_2 per mass of biochar produced (EF_{CO2}) by dividing by the molar mass ratio of C and CO_2. The amount of flue gas released per mass of biochar produced ($V_{flue\ gas}$) can then be calculated by relating EF_{CO2} to the measured concentration of CO_2 in flue gas ($conc_{CO2}$):

$$V_{flue\ gas} = \frac{EF_{CO2}}{conc_{CO2}} \quad \text{Eq. 6}$$

Finally, EF_{PFAS} can be computed using $V_{flue\ gas}$ and the measured concentration of a given PFAS:

$$EF_{PFAS} = conc_{PFAS} \times V_{flue\ gas} \quad \text{Eq. 7}$$

A mass balance for PFAS upon the pyrolysis of 1 tonne of each feedstock is set up based on total concentrations of PFAS in the feedstock and resulting biochar (adjusted by biochar yield) and emission factors for total PFAS. Only feedstocks and treatments for which biochar and emission data was available were included in the analysis (Table 1). No data on PFAS in the pyrolysis oil condensed from the syngas was acquired, since the extraction of PFAS from this matrix entailed analytical challenges that would not ensure the quality of the results; pyrolysis oil is a strongly acidic mixture of water, organic acids, phenols, alcohols, and complex high molecular mass organic compounds (Papari & Hawboldt, 2018). The fraction not found in biochar or exhaust is therefore considered to be either decomposed or in the pyrolysis oil.

3. Results and discussion

3.1 PFAS in feedstocks

In total, 26 out of the 41 PFAS-congeners analysed for using method AA were detected across the eight feedstocks (see Figure 1, Table S.5), in concentrations ranging from 56 to 3651 ng g^{-1}. In addition, using method BB for two of the sewage sludge feedstocks (DSS-1 and DSS-2), 3 of the 11 additional precursor compounds were detected, but no ultrashort chain PFAS were detected (method BC). The sewage sludge feedstocks presented the largest variety of PFAS congeners: 9, 12, 10 and 9 different PFAS-congeners were detected in DSS-1, DSS-2, LSS, and DWSS respectively (Figure 2). Eight congeners were detected in the food waste reject. Few congeners were detected in the wood-based feedstocks (five in WT, two in GW and five in CWC).

Sewage sludge feedstocks. The total amounts of PFAS ($PFAS_{tot}$) in the sewage sludge feedstocks were 56 ± 11, 441 ± 33, 340 ± 43 and 214 ± 88 ng g^{-1} for the DSS-1, DSS-2, LSS and DWSS respectively. These concentrations are similar to previously reported findings: 125-809 ng g^{-1} in 25 WWTPs in Shanghai (Yan et al., 2012), 5.2-150 ng g^{-1} in 14 WWTPs across Australia (Gallen et al., 2018), 5.6 to 963.2 ng g^{-1} in 43 WWTPs in Czech Republic (Semerád et al., 2020), and 193-502 ng g^{-1} in biosolids from WWTPs from the Greater Chicago area (Sepulvado et al., 2011). The distribution of PFAS in the sewage sludge feedstocks (Figure 1), DSS-1, DSS-2, LSS and DWSS, were mainly dominated by PFPeA (0, 76.3, 63.8. and 0 % of $PFAS_{tot}$ respectively), followed by PFOS (25.4, 8.6, 3.8 and 16.2 % of $PFAS_{tot}$ respectively) and 4:2 FTS (43.7, 6.2, 18.8 and 37.3 % of $PFAS_{tot}$ respectively). Additionally, PFBA constituted 40 % of the $PFAS_{tot}$ in the DWSS, but was not detected in the other sludge feedstock samples. The DSS-2 and DWSS feedstocks were collected from WWTPs receiving runoff from firefighting training sites, which are impacted by legacy AFFF. The PFAS that dominate these feedstocks (PFBA, PFPeA, PFOS and 4:2 FTS) have all been found in soils and groundwater impacted by AFFF (Anderson et al., 2016; Høisæter et al., 2019). In addition, sewage sludges contain a wide range of PFAS compounds derived from their extensive use in both households and industries contaminated by PFAS originating from cosmetics, detergents, washing of textiles and the items with surface coatings (Munoz et al., 2022).

Wood-based feedstocks. The highest $PFAS_{tot}$ concentration was found in the wood chips feedstock (3651 ± 1846 ng g^{-1}), strongly dominated by the presence of PFHxA (98%). PFHxA is a surfactant typically found in high concentrations in AFFF (Ahrens et al., 2015; Buck et al., 2011; Herzke et al., 2012), but also in textiles (Rodgers et al., 2022) and fluoropolymer production (Wang et al., 2014). The other wood-based feedstocks, waste timber (WT) and garden waste (GW), were also dominated by PFHxA (Figure 1). PFCAs have previously been found in wood composite building materials at concentrations up to 24.5 ng g^{-1} (Bečanová et al., 2016). As waste timber contains demolition wood, such materials are likely present. Diffuse PFAS contamination in soil and water is taken up in plants, particularly short chain PFCAs (Ghisi et al., 2019), thus PFAS in garden waste could stem from the vegetation itself. This could also be the case for the wood chips, but due to the high concentration (3651 ± 1846 ng g^{-1}, confirmed by a triplicate sample) contamination in the production chain of the wood chip pellets is also a strong possibility.

Food waste reject feedstock. The second highest $PFAS_{tot}$ feedstock concentration was found in the food waste reject (FWR, 676 ± 62 ng g^{-1}), which was dominated by PFBA (32.3% of $PFAS_{tot}$), PFPeA (31.8% of $PFAS_{tot}$) and 4:2 FTS (33.0% of $PFAS_{tot}$). PFBA was previously detected in food packaging materials (Zafeiraki et al., 2014) , and PFBA and PFPeA were both found in water proofing agents and non-stick ware (Herzke et al., 2012), which are components related to the processing and packaging of food. Furthermore, the contamination in the food waste might derive from the food itself as several studies have shown uptake of various PFAS into agricultural plants such as corn, oats, rye and wheat, as a result of soil contamination or PFAS-contaminated sewage sludge application (Ghisi et al., 2019).

On the whole, the large concentration range (56-3651 ng g^{-1} $PFAS_{tot}$) and wide variety of PFAS-congeners (28 congeners) (Figure 1) make the selected feedstocks well suited to demonstrate the effect of pyrolysis as a waste handling method for PFAS-contaminated organic waste, as the effect of thermal degradation of PFAS depends both upon total concentration and PFAS-type (Alinezhad et al., 2022).

462

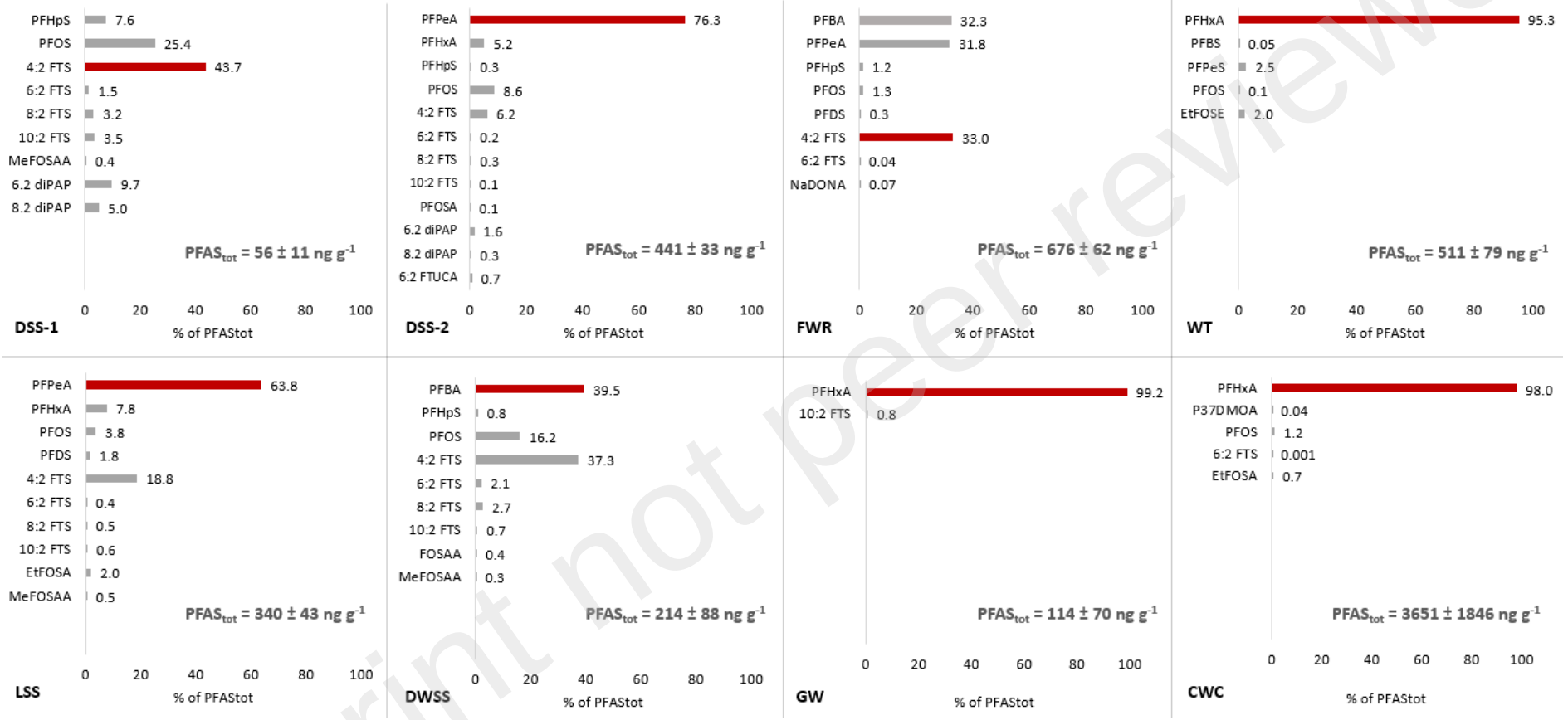

463 *Figure 1. Total concentration ($PFAS_{tot}$ ng g^{-1}) and distribution (% of $PFAS_{tot}$) of PFAS compounds detected in the digested sewage sludge (DSS-1 and DSS-2),*
464 *limed sewage sludge (LSS) de-watered sewage sludge (DWSS), food waste reject (FWR), waste timber (WT), garden waste (GW), and wood chips (CWC) prior*
465 *to pyrolysis treatment.*

3.2 PFAS in biochars

Concentrations of $PFAS_{tot}$ in the biochar samples ranged between <LOD and 3.4 ng g^{-1} (Figure 2, Table S.5) and were thus 1-3 orders of magnitude less than the concentrations in the original feedstocks (details about removal efficiency in section 3.3, Table S.7). There was no statistically significant ($p>0.05$) linear reduction in PFAS concentration with pyrolysis temperature. However, biochars produced at 500 ºC had the highest $PFAS_{tot}$ concentrations (1 – 3.4 ng g^{-1}), except for WT biochar where no PFAS was detected (Table S.5). Meanwhile, no PFAS were detected in biochars produced at 800 ºC. To the best of our knowledge, attempts to detect residual PFAS concentrations in biochar have previously only been made in pilot studies by Thoma et al. (2022) and Kundu et al. (2021). In the former, PFAS in sewage sludge (biosolids) and resulting biochars from two commercial pyrolysis plants run at around 600 ºC were investigated. They reported PFOS and PFOA (0.5 and 0.2 ng g^{-1} respectively), at concentrations 10 times lower than what was found in the present work. In the latter, sewage sludge was pyrolyzed at 500 and 600 °C to in a semi pilot scale unit, but the biochars produced had non-detectable concentrations (LODs not provided). In both these studies however, little or no details were provided about the analytical methods used.

Pyrolysis reduced the variety of PFAS congeners – the biochar samples contained 60-100% fewer congeners than their feedstock materials (Tables S.5). Alinezhad et al. (2022) found that polyfluorinated compounds, such as FTS and FSA are more easily degraded than PFCA and PFSA, with the PFSAs being the most persistent. The trend of PFSAs and PFCAs being the most stable is also visible in the present study, as these groups of congeners made up 100% of PFAS detected in biochars (PFPeA, PFHxA, PFOA, PFNA, PFHpS, PFOS and P37DMOA), except for trace amounts of 6:2 FTS (0.04-0.14 ng g^{-1}) found in some of the WT (600 °C), GW (500 and 600 °C) and CWC (500, 600 and 700 °C) biochars, and 6:2 FTUCA (0.4±0.2 in ng g^{-1}) in DSS-2 at 500 ºC (Table S.5). While short chain PFAS (≤6 CF_2-moieties) dominated PFAS presence in feedstock samples (Figure 1; median fraction of short chain PFAS was 95% across the eight feedstocks (Table S.5)) a shift towards long chain PFAS (>6 CF_2-moieties) was observed for the biochars. Across all biochars in which PFAS were detected, the median fraction of long chain PFAS was 99% (Table S.5). No ultrashort

chain PFAS compounds were detected in the biochars. This apparent higher persistence of long chain PFAS to thermal degradation compared to short chain ones is corroborated by Xiao et al. (2020) who observed a decreasing thermal stability of PFCAs with decreasing tail length when studying the regeneration of spent activated carbon through thermal decomposition.

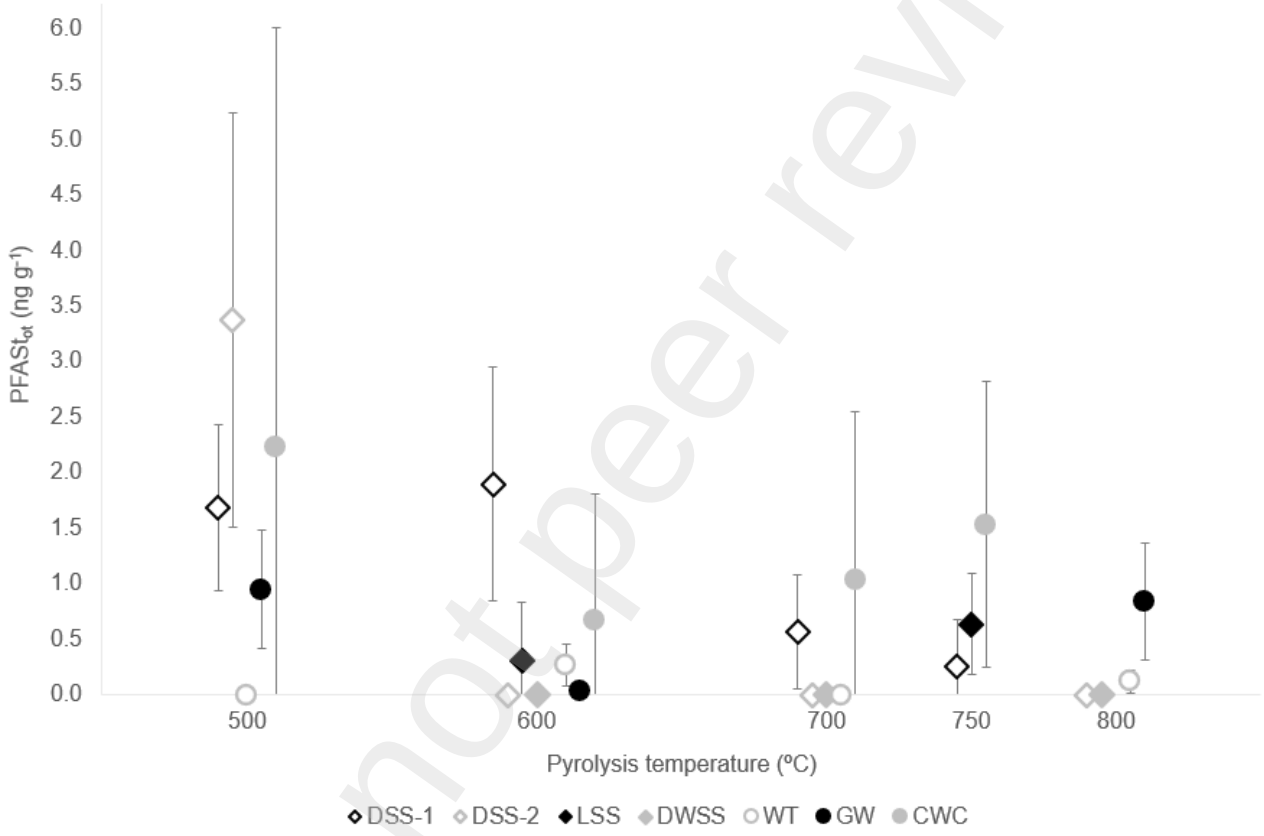

Figure 2. Total PFAS (PFAS$_{tot}$, ng g^{-1}) in biochars produced at various pyrolysis temperatures (500-800 ºC) from the digested sewage sludge (DSS-1 and DSS-2), limed sewage sludge (LSS), de-watered sewage sludge (DWSS), food waste reject (FWR), waste timber (WT), garden waste (GW), and wood chips (CWC). Data points and error bars are showing the mean and standard deviations from triplicate analysis.

3.3 PFAS Removal Efficiencies

Removal efficiencies (RE) for PFAS$_{tot}$ were larger than or equal to 98% (Table S.7) across all treatment temperatures (500-800 ºC) and feedstocks (sludge and wood based). Note that RE (Eq 2) is

corrected by biochar yield to consider mass reduction (2-5 times original mass, Table S.6) during the pyrolysis process. The lowest REs were recorded for DSS-1 at 500 ºC and 600 ºC (98.4% and 98.3%, respectively). At treatment temperatures ≥700 ºC however, more than 99% of $PFAS_{tot}$ was removed from all feedstocks. These results are in agreement with Alinezhad et al. (2022) who presented the decomposition of PFAS in soil under thermal treatments, demonstrating that RE after pyrolysis at 500 ºC and residence time of 30 min was above 99%, regardless of PFAS initial load and type. In the present study, the residence time applied in the pyrolysis experiments was 20 min. It could be possible that by increasing the residence time, higher RE% would have been obtained. The latter hypothesis can be supported by the observations for DWSS feedstock, for which a residence time of 40 min was applied, resulting in REs of 100% for all treatment temperatures (600-800 ºC).

The somewhat lower RE recorded for DSS-1 compared to the other feedstocks is probably due to the DSS-1 feedstock having a relatively large amount of the long chain sulfonate, PFOS (14 ng g^{-1}, 25.4% of $PFAS_{tot}$) that appeared to be more persistent towards thermal degradation (Alinezhad et al., 2022) than the short chain PFAS that dominated some of the other feedstocks (see section 3.2 for more details).

Overall, the temperatures required to achieve REs ~100% for PFAS being higher than 600 °C is similar to or higher than reported for other organic contaminants as Moško et al. (2021) demonstrated for pharmaceuticals, PCBs, PAHs and endocrine disrupting and hormonal compounds, in sewage sludge pyrolysis.. For organophosphate flame retardants (OPFRs), as documented in a parallel study by our group using the same samples (Castro et al., submitted), pyrolysis temperatures ≥500 C were sufficient to achieve REs ~100%. The relative persistence to thermal degradation of PFAS compared to other organic contaminants is however expected, due to the high energy of the C-F bond relative to that of C-C and C-Cl bonds (O'Hagan, 2008). Nonetheless, an important caveat to these results is that several non-target PFAS (i.e. PFAS other than the 56 analysed for) may have been produced, such as per and polyfluorinated alkanes and alkenes with and without a head group (Alinezhad et al., 2022; Yao et al., 2022).

3.4 PFAS Emission Factors

PFAS were detected in the flue gas (post syngas combustion) from the pyrolysis of the sewage sludge feedstocks at all treatment temperatures (Table 2), demonstrating that pyrolysis at ≥500 ºC coupled with syngas combustion at 800-900 ºC does not fully decompose PFAS present in the original feedstock. This is corroborated by Thoma et al. (2022) who detected PFAS in flue gas scrubber water of pyrolysis units run at 600 °C with syngas combustion at 1020 °C. Total PFAS-concentrations in the exhaust, both particle and gaseous fractions included, ranged from <LOD to 100 ng m^{-3} with a mean concentration of 50 ± 70 ng m^{-3}. The mean concentration of gaseous PFAS (40 ± 61 ng m^{-3}) was somewhat higher than the particle based PFAS (10 ± 11 ng m^{-3}), but samples from both fractions demonstrated high heterogeneity (large standard deviations).

Unlike the biochar samples however, where long chain PFAS dominated (Tables S.5), as he majority (60%) of all PFAS detected in the exhaust, particle-bound and gaseous alike, were short chain PFAS. The two carboxylic acids with 3 and 4 CF_2-moieties, PFBA and PFPeA, and the sulfonic acid with 4 CF_2-moieties, PFBS, comprised 44-100% of all PFAS detected in the exhaust, despite not being detected in the feedstock pyrolyzed. This suggests that long chain PFAS in the feedstocks are decomposed to short chain PFAS in the pyrolysis reactor and/or combustion chamber. This observation is supported by Yao et al. (2022), who suggested radical mediated chain scission either at the functional head or at random sites along the chain as the most probable thermal degradation pathway for PFAS. Ultrashort chain PFAS compounds were, however, not detected in the gaseous phase of the flue gas (they were not analysed for in the particle phase due to practical difficulties).

Calculated $EF_{PFAStot}$ (Eq. 7) show that a range of 0.01 – 3.1 mg of $PFAS_{tot}$ were emitted per tonne of biochar produced from the sewage sludges studied (Table 2). EF_{PFAS} for all single PFAS compounds detected are compiled in Table S.9 and the calculated volumes of syngas used to derive these factors are shown in Table S.10. To the authors' knowledge, EF_{PFAS} have never been reported, either for dry pyrolysis or full scale waste incineration plants (Stoiber et al., 2020). Thus, there is no literature to compare the present results to. The EF_{PFAS} are about 10-1000 times lower than emission factors for polycyclic aromatic hydrocarbons (PAHs) from the pyrolysis of waste timber at 600 ºC, as

previously documented by our group (Sørmo et al., 2020). However, it is expected that PAH emissions should largely exceed PFAS emissions, as these compounds can be generated from carbon matrices during pyrolysis and combustion (Mastral & Callén, 2000).

570 *Table 2. Emission concentrations (ng m^{-3}) for PFAS detected in flue gas from the pyrolysis of digested sewage sludge (DSS-1 and DSS-2) and limed sewage*
571 *sludge (LSS), along with the relative fractions of total PFAS found in the gaseous and particle-based fractions (%). Emission factors (EF, mg $tonne^{-1}$) for*
572 *total PFAS also shown. Concentrations and EF shown as mean ± standard deviation.*

Metric	PFAS type	PFAS compound	DSS-1			DSS-2				LSS	
			500	600	700	500	600	700	800	600	750
Emission concentrations (ng m^{-3})	PFCA	PFBA	n.d.	10.76 ± 0.02	11.5 ± 0.4	n.d.	3.6 ± 0.2	7.4 ± 0.5	9 ± 1	9.4 ± 0.5	12 ± 2
		PFPeA	2.0 ± 0.4	26 ± 36	n.d.	n.d.	9 ± 15	n.d.	n.d.	n.d.	n.d.
		PFHpA	n.d.	100 ± 99	35 ± 61	n.d.	n.d.	n.d.	n.d.	n.d.	n.d.
		7H-PFHpA	n.d.	22 ± 27	n.d.	n.d.	n.d.	n.d.	n.d.	n.d.	n.d.
	PFSA	PFBS	42 ± 10	58 ± 16	46 ± 6	n.d.	n.d.	n.d.	10.9 ± 0.8	0.19 ± 0.03	n.d.
			n.d.	n.d.	n.d.	0.6 ± 0.8	n.d.	n.d.	n.d.	n.d.	n.d.
	FTS	6:2 FTS	n.d.	n.d.	0.03 ± 0.05	n.d.	n.d.	n.d.	n.d.	n.d.	n.d.
		8:2 FTS	n.d.	n.d.	n.d.	n.d.	8 ± 14	n.d.	n.d.	n.d.	n.d.
	FSA	PFOSA	n.d.	n.d.	n.d.	n.d.	6 ± 11	n.d.	n.d.	n.d.	n.d.
		MeFOSAA	11 ± 19	n.d.	n.d.	n.d.	n.d.	n.d.	n.d.	n.d.	n.d.
	Misc.	NaDONA	5 ± 9	n.d.	3 ± 6	n.d.	n.d.	n.d.	n.d.	n.d.	n.d.
	Sum	$PFASt_{ot}$	**59** ± 23	**217** ± 110	**96** ± 62	**0.6** ± 0.8	**27** ± 23	**7.4** ± 0.5	**20** ± 1	**9.6** ± 0.5	**12** ± 2
	Sum	Gaseous (%)	97	94	88	0	87	0	55	0	0
		Particles (%)	**3**	**6**	**12**	**100**	**13**	**100**	**45**	**100**	**100**
EF (mg $tonne^{-1}$)	Sum	$PFAS_{tot}$	0.2 ± 0.1	3.1 ± 1.6	1.2 ± 0.8	0.01 ± 0.02	0.9 ± 0.8	0.32 ± 0.02	0.7 ± 0.1	0.0096 ± 0.0005	0.9 ± 0.2

3.5 PFAS Mass Balance using pyrolysis as a waste treatment option

The potential of pyrolysis as a waste treatment alternative was assessed through the mass balance of total PFAS in the pyrolysis treatment of 1 tonne of feedstock. Three feedstocks (DSS-1, DSS-2 and LSS) and the pyrolysis temperatures applied in their treatments (500 – 800 ºC) were considered. Of the total amount of PFAS present in the feedstocks, a small fraction ends up in the biochar (<2%) regardless of pyrolysis temperature and feedstock, as is also reflected by the calculated removal efficiencies (Table S.7). However, regarding emissions themselves, a similarly small fraction is released with flue gas through the chimney (<3 %). This means that the large majority of PFAS (>95%) in the feedstocks is either decomposed in the pyrolysis reactor or in the combustion chamber, and/or trapped in the pyrolysis oil.

The mass balance varied somewhat with pyrolysis temperature, but it appeared that the factor that affects the distribution the most, is the composition of PFAS congeners in the feedstock. The DSS-1 sample, with a relatively high concentration of the persistent PFOS (14±4 ng g^{-1}), pyrolyzed at 600 °C can be considered as a worst-case scenario, for which 1.73% would end up in the biochar, 2.81% would be emitted and 95.47% would be decomposed (Table S.11). A best-case scenario on the other hand would be the pyrolysis of the DSS-2 feedstock, which has almost a 10 times higher concentration in the feedstock, but which is dominated by short chain PFCAs and FTS (Figure 2). Pyrolyzing the DSS-2 feedstock at 600 °C, would result in 0.00% ending up in the biochar, 0.08% being emitted and 99.92% being decomposed. Considering the fact that most options for handling PFAS-containing waste lead to some sort of emission, either through flue gas, landfill leachate or soil runoff (Stoiber et al., 2020), the relatively large amount that is decomposed using the pyrolysis approach could be worth the emissions caused, especially if emissions can be lowered, e.g. by optimizing the pyrolysis process for PFAS removal, or more simply by a filter solution.

As some of the feedstock and temperature treatment combinations yielded high particle-based emissions (up to 100%, Table 2) it is expected that emissions can be reduced by introducing a flue gas scrubber, an established technology for waste incineration. Wet scrubbers are especially efficient for scenarios when the target contaminants are associated with particles, as reported by Choi et al. (2007)

who demonstrated a reduction of 90% in emissions of dioxins from waste incinerators with high particle loads. Thoma et al. (2022) did not quantify PFAS-emissions, but detected PFAS in water from wet scrubbing of exhaust during the pyrolysis of sewage sludge, thereby indicating scavenging of PFAS compounds from the flue gas. Thus, there is a need to properly document the effect of flue gas cleaning technology on PFAS-emissions from pyrolysis. It is also important to note that the present work accounts for emissions of a wide range of PFAS-congeners and precursor compounds, but has not documented the release of other possible thermal degradation products identified in laboratory studies, such as perfluoroalkanes, perfluoroalkenes, perfluoralkyl aldehydes and fluorotelomere alcohols (Alinezhad et al., 2022; Yao et al., 2022). The presence of said compounds in exhaust from commercial pyrolysis units could be challenging to document due to the need for advanced technology such as online gas chromatography systems. A first approach could therefore be to assess the environmental risk related to the emissions of potential degradation products identified in laboratory studies.

There is also a need to quantify PFAS in pyrolysis oil. This fraction contains both water and organic oily liquids, with the interface between those potentially acting as a scavenging phase for surface-active PFAS compounds. As the majority of PFAS (>95%) is either trapped in this fraction or transformed into decomposition products in the flue gas, the content of PFAS in the pyrolysis oil could reveal more about the extent of decomposition products in the flue gas. If a significant amount of PFAS is not decomposed, but present in the pyrolysis oil, the oil will have to be handled/used in such a way that further emissions will not occur. At the local level, the pyrolysis oil and syngas could themselves be combusted as a heat source on site, including for the heating of the pyrolysis unit itself, which would further destroy the residual PFAS.

4. Conclusions

The present work has demonstrated dry pyrolysis has potential as a waste handling alternative for PFAS-contaminated organic waste. For optimization towards PFAS removal, an adequately high pyrolysis temperature and residence time must be used. Considering the results from the present and previous works, pyrolysis of contaminated organic waste should be run at a minimum of 600 °C in order to properly decompose PFAS and other organic contaminants to non-detectable levels.

The nature of the feedstock and the type of PFAS present in the samples should also be considered, as removal efficiencies differed among the different feedstock pyrolyzed. Long chain PFAS appeared more challenging to degrade. Therefore, pyrolysis conditions should be adjusted to individual feedstocks. These conclusions confirm hypothesis one, which stated that PFAS would be decomposed regardless of initial load given a high enough pyrolysis temperature. However, optimization towards a specific feedstock might allow for using a lower pyrolysis temperature or residence time that reduces the energy demand for the process and the biochar yield.

It was furthermore demonstrated that the fraction of PFAS in the original organic wastes that ends up being released with the flue gas is relatively low (<3%). This supports the second hypothesis, that a mass balance would reveal that the majority of quantifiable PFAS will be decomposed in the pyrolysis process. Even though the emissions make up a small fraction of the total mass of PFAS being treated, the total emissions from large-scale operations could be significant. Considering that the complete presence and nature of degradation products in the flue gas is unknown, flue gas cleaning might be necessary to avoid PFAS compounds being cycled back into the environment.

PFAS decomposition seems to be a motivation for adopting dry pyrolysis as a waste handling option; however, future studies should also consider other contaminants and externalities, such as life cycle impacts compared to the status quo options of sending the contaminated feedstocks to incinerators, landfills, or to be used as fertilizer in agricultural areas.

Acknowledgements

The authors acknowledge funding from the Research Council of Norway, through the joint-industry sustainability (BIA-X) project "Valorization of Organic Waste" (VOW) (NFR 299070) and the Miljøforsk project SLUDGEFFECT (NFR 302371); and from the European Union's Horizon 2020 research and innovation programme under the Marie Skłodowska-Curie Action grant agreement No 860665 (PERFORCE3 Innovative Training Network). Natalia Kasian, Gudny Flatabø, Hartantyo Seto Guntoro, Aadam Maczko and Bendik Bache Hansen from Scanship are acknowledged for assisting in biochar production, Caroline Berge Hansen, Gabrielle Dublet Adli and Maren Valestrand Tjønneland at NGI for contributing to field work and Irene E. Eriksen Dahl for biochar elemental analysis at NMBU. The PFAS analysis (method AA) was carried out in the EnviroChemistry Lab at NTNU, and at the Institute for Analytical Research, HSF (method BB and BC).

References

Abunada, Z.-A., Motasem Y. D. AU-Bashir, Mohammed J. K. TI-An Overview of Per-and Polyfluoroalkyl Substances (PFAS) in the Environment: Source, Fate, Risk and Regulations. (2020). *Water*, *12*(12). https://doi.org/10.3390/w12123590

Ahmad, M., Rajapaksha, A. U., Lim, J. E., Zhang, M., Bolan, N., Mohan, D., Vithanage, M., Lee, S. S., & Ok, Y. S. (2014). Biochar as a sorbent for contaminant management in soil and water: A review. *Chemosphere*, *99*, 19–33. https://doi.org/10.1016/j.chemosphere.2013.10.071

Ahmadireskety, A., Da Silva, B. F., Townsend, T. G., Yost, R. A., Solo-Gabriele, H. M., & Bowden, J. A. (2021). Evaluation of extraction workflows for quantitative analysis of per- and polyfluoroalkyl substances: A case study using soil adjacent to a landfill. *Science of The Total Environment*, *760*, 143944. https://doi.org/10.1016/j.scitotenv.2020.143944

Ahrens, L., Norström, K., Viktor, T., Cousins, A. P., & Josefsson, S. (2015). Stockholm Arlanda Airport as a source of per- and polyfluoroalkyl substances to water, sediment and fish. *Chemosphere*, *129*, 33–38. https://doi.org/10.1016/j.chemosphere.2014.03.136

676 Alhashimi, H. A., & Aktas, C. B. (2017). Life cycle environmental and economic performance of
677 biochar compared with activated carbon: A meta-analysis. *Resources, Conservation and*
678 *Recycling*, *118*, 13–26. https://doi.org/10.1016/j.resconrec.2016.11.016
679 Alinezhad, A., Challa Sasi, P., Zhang, P., Yao, B., Kubátová, A., Golovko, S. A., Golovko, M. Y., & Xiao,
680 F. (2022). An Investigation of Thermal Air Degradation and Pyrolysis of Per- and
681 Polyfluoroalkyl Substances and Aqueous Film-Forming Foams in Soil. *ACS ES&T Engineering*,
682 *2*(2), 198–209. https://doi.org/10.1021/acsestengg.1c00335
683 Allred, B. M., Lang, J. R., Barlaz, M. A., & Field, J. A. (2015). Physical and Biological Release of Poly-
684 and Perfluoroalkyl Substances (PFASs) from Municipal Solid Waste in Anaerobic Model
685 Landfill Reactors. *Environmental Science & Technology*, *49*(13), 7648–7656.
686 https://doi.org/10.1021/acs.est.5b01040
687 Anderson, R. H., Long, G. C., Porter, R. C., & Anderson, J. K. (2016). Occurrence of select
688 perfluoroalkyl substances at U.S. Air Force aqueous film-forming foam release sites other
689 than fire-training areas: Field-validation of critical fate and transport properties.
690 *Chemosphere*, *150*, 678–685. https://doi.org/10.1016/j.chemosphere.2016.01.014
691 Asimakopoulos, A. G., Wang, L., Thomaidis, N. S., & Kannan, K. (2014). A multi-class bioanalytical
692 methodology for the determination of bisphenol A diglycidyl ethers, p-hydroxybenzoic acid
693 esters, benzophenone-type ultraviolet filters, triclosan, and triclocarban in human urine by
694 liquid chromatography–tandem mass spectrometry. *Journal of Chromatography A*, *1324*,
695 141–148. https://doi.org/10.1016/j.chroma.2013.11.031
696 Ateia, M., Maroli, A., Tharayil, N., & Karanfil, T. (2019). The overlooked short- and ultrashort-chain
697 poly- and perfluorinated substances: A review. *Chemosphere*, *220*, 866–882.
698 https://doi.org/10.1016/j.chemosphere.2018.12.186
699 Bailis, R., Ezzati, M., & Kammen, D. M. (2003). Greenhouse gas implications of household energy
700 technology in Kenya. *Environmental Science & Technology*, *37*(10), 2051–2059.

701 Barber, J. L., Berger, U., Chaemfa, C., Huber, S., Jahnke, A., Temme, C., & Jones, K. C. (2007). Analysis
702 of per- and polyfluorinated alkyl substances in air samples from Northwest Europe. *Journal*
703 *of Environmental Monitoring*, *9*(6), 530–541. https://doi.org/10.1039/B701417A
704 Barry, D., Barbiero, C., Briens, C., & Berruti, F. (2019). Pyrolysis as an economical and ecological
705 treatment option for municipal sewage sludge. *Biomass and Bioenergy*, *122*, 472–480.
706 https://doi.org/10.1016/j.biombioe.2019.01.041
707 Bečanová, J., Melymuk, L., Vojta, Š., Komprdová, K., & Klánová, J. (2016). Screening for perfluoroalkyl
708 acids in consumer products, building materials and wastes. *Chemosphere*, *164*, 322–329.
709 https://doi.org/10.1016/j.chemosphere.2016.08.112
710 Beesley, L., Moreno-Jiménez, E., Gomez-Eyles, J. L., Harris, E., Robinson, B., & Sizmur, T. (2011). A
711 review of biochars' potential role in the remediation, revegetation and restoration of
712 contaminated soils. *Environmental Pollution*, *159*(12), 3269–3282.
713 https://doi.org/10.1016/j.envpol.2011.07.023
714 Berg, C., Crone, B., Gullett, B., Higuchi, M., Krause, M. J., Lemieux, P. M., Martin, T., Shields, E. P.,
715 Struble, E., Thoma, E., & Whitehill, A. (2022). Developing innovative treatment technologies
716 for PFAS-containing wastes. *Journal of the Air & Waste Management Association*, *72*(6),
717 540–555. https://doi.org/10.1080/10962247.2021.2000903
718 Block, C., Van Caneghem, J., Van Brecht, A., Wauters, G., & Vandecasteele, C. (2015). Incineration of
719 Hazardous Waste: A Sustainable Process? *Waste and Biomass Valorization*, *6*(2), 137–145.
720 https://doi.org/10.1007/s12649-014-9334-3
721 Buck, R. C., Franklin, J., Berger, U., Conder, J. M., Cousins, I. T., de Voogt, P., Jensen, A. A., Kannan, K.,
722 Mabury, S. A., & van Leeuwen, S. P. (2011). Perfluoroalkyl and polyfluoroalkyl substances in
723 the environment: Terminology, classification, and origins. *Integrated Environmental*
724 *Assessment and Management*, *7*(4), 513–541. https://doi.org/10.1002/ieam.258

725 Choi, K.-I., & Lee, D.-H. (2007). PCDD/DF concentrations at the inlets and outlets of wet scrubbers in
726 Korean waste incinerators. *Chemosphere*, *66*(2), 370–376.
727 https://doi.org/10.1016/j.chemosphere.2006.04.094
728 Cornelissen, G., Pandit, N. R., Taylor, P., Pandit, B. H., Sparrevik, M., & Schmidt, H. P. (2016).
729 Emissions and Char Quality of Flame-Curtain 'Kon Tiki' Kilns for Farmer-Scale
730 Charcoal/Biochar Production. *PLOS ONE*, *11*(5), e0154617.
731 https://doi.org/10.1371/journal.pone.0154617
732 Dempsey, C. R., & Oppelt, E. T. (1993). Incineration of Hazardous Waste: A Critical Review Update.
733 *Air & Waste*, *43*(1), 25–73. https://doi.org/10.1080/1073161X.1993.10467116
734 Gallen, C., Eaglesham, G., Drage, D., Nguyen, T. H., & Mueller, J. F. (2018). A mass estimate of
735 perfluoroalkyl substance (PFAS) release from Australian wastewater treatment plants.
736 *Chemosphere*, *208*, 975–983. https://doi.org/10.1016/j.chemosphere.2018.06.024
737 Ghisi, R., Vamerali, T., & Manzetti, S. (2019). Accumulation of perfluorinated alkyl substances (PFAS)
738 in agricultural plants: A review. *Environmental Research*, *169*, 326–341.
739 https://doi.org/10.1016/j.envres.2018.10.023
740 Glüge, J., Scheringer, M., Cousins, I. T., DeWitt, J. C., Goldenman, G., Herzke, D., Lohmann, R., Ng, C.
741 A., Trier, X., & Wang, Z. (2020). An overview of the uses of per- and polyfluoroalkyl
742 substances (PFAS). *Environmental Science: Processes & Impacts*, *22*(12), 2345–2373.
743 https://doi.org/10.1039/D0EM00291G
744 Gupta, S., & Kua, H. W. (2019). Carbonaceous micro-filler for cement: Effect of particle size and
745 dosage of biochar on fresh and hardened properties of cement mortar. *Science of The Total*
746 *Environment*, *662*, 952–962. https://doi.org/10.1016/j.scitotenv.2019.01.269
747 Hale, S. E., Arp, H. P. H., Kupryianchyk, D., & Cornelissen, G. (2016). A synthesis of parameters
748 related to the binding of neutral organic compounds to charcoal. *Chemosphere*, *144*, 65–74.
749 https://doi.org/10.1016/j.chemosphere.2015.08.047

Hale, S. E., Kalantzi, O. I., & Arp, H. P. H. (2022). Introducing the EU project ZeroPM: zero pollution of persistent, mobile substances. *Environmental Sciences Europe*, *34*(1), 108. https://doi.org/10.1186/s12302-022-00681-5

Hale, S. E., Nurida, N. L., Jubaedah, Mulder, J., Sørmo, E., Silvani, L., Abiven, S., Joseph, S., Taherymoosavi, S., & Cornelissen, G. (2020). The effect of biochar, lime and ash on maize yield in a long-term field trial in a Ultisol in the humid tropics. *Science of The Total Environment*, *719*, 137455. https://doi.org/10.1016/j.scitotenv.2020.137455

Herzke, D., Olsson, E., & Posner, S. (2012). Perfluoroalkyl and polyfluoroalkyl substances (PFASs) in consumer products in Norway – A pilot study. *Chemosphere*, *88*(8), 980–987. https://doi.org/10.1016/j.chemosphere.2012.03.035

Høisæter, Å., Pfaff, A., & Breedveld, G. D. (2019). Leaching and transport of PFAS from aqueous film-forming foam (AFFF) in the unsaturated soil at a firefighting training facility under cold climatic conditions. *Journal of Contaminant Hydrology*, *222*, 112–122. https://doi.org/10.1016/j.jconhyd.2019.02.010

Ippolito, J. A., Spokas, K. A., Novak, J. M., Lentz, R. D., & Cantrell, K. B. (2015). Biochar elemental composition and factors influencing nutrient retention. In *Biochar for Environmental Management: Science, Technology and Implementation* (2nd ed.). Routledge.

Krafft, M. P., & Riess, J. G. (2015). Per- and polyfluorinated substances (PFASs): Environmental challenges. *Current Opinion in Colloid & Interface Science*, *20*(3), 192–212. https://doi.org/10.1016/j.cocis.2015.07.004

Kundu, S., Patel, S., Halder, P., Patel, T., Hedayati Marzbali, M., Pramanik, B. K., Paz-Ferreiro, J., de Figueiredo, C. C., Bergmann, D., Surapaneni, A., Megharaj, M., & Shah, K. (2021). Removal of PFASs from biosolids using a semi-pilot scale pyrolysis reactor and the application of biosolids derived biochar for the removal of PFASs from contaminated water. *Environmental Science: Water Research & Technology*, *7*(3), 638–649. https://doi.org/10.1039/D0EW00763C

776 Lang, J. R., Allred, B. M., Field, J. A., Levis, J. W., & Barlaz, M. A. (2017). National Estimate of Per- and
777 Polyfluoroalkyl Substance (PFAS) Release to U.S. Municipal Landfill Leachate. *Environmental*
778 *Science & Technology*, *51*(4), 2197–2205. https://doi.org/10.1021/acs.est.6b05005
779 Lehmann, J., Gaunt, J., & Rondon, M. (2006). Bio-char Sequestration in Terrestrial Ecosystems – A
780 Review. *Mitigation and Adaptation Strategies for Global Change*, *11*(2), 403–427.
781 https://doi.org/10.1007/s11027-005-9006-5
782 Li, L., Zou, D., Xiao, Z., Zeng, X., Zhang, L., Jiang, L., Wang, A., Ge, D., Zhang, G., & Liu, F. (2019).
783 Biochar as a sorbent for emerging contaminants enables improvements in waste
784 management and sustainable resource use. *Journal of Cleaner Production*, *210*, 1324–1342.
785 https://doi.org/10.1016/j.jclepro.2018.11.087
786 Mastral, A. M., & Callén, M. S. (2000). A Review on Polycyclic Aromatic Hydrocarbon (PAH) Emissions
787 from Energy Generation. *Environmental Science & Technology*, *34*(15), 3051–3057.
788 https://doi.org/10.1021/es001028d
789 Moško, J., Pohořelý, M., Cajthaml, T., Jeremiáš, M., Robles-Aguilar, A. A., Skoblia, S., Beňo, Z.,
790 Innemanová, P., Linhartová, L., Michalíková, K., & Meers, E. (2021). Effect of pyrolysis
791 temperature on removal of organic pollutants present in anaerobically stabilized sewage
792 sludge. *Chemosphere*, *265*, 129082. https://doi.org/10.1016/j.chemosphere.2020.129082
793 Munoz, G., Michaud, A. M., Liu, M., Vo Duy, S., Montenach, D., Resseguier, C., Watteau, F., Sappin-
794 Didier, V., Feder, F., Morvan, T., Houot, S., Desrosiers, M., Liu, J., & Sauvé, S. (2022). Target
795 and Nontarget Screening of PFAS in Biosolids, Composts, and Other Organic Waste Products
796 for Land Application in France. *Environmental Science & Technology*, *56*(10), 6056–6068.
797 https://doi.org/10.1021/acs.est.1c03697
798 Nelson, D. W., & Sommers, L. E. (1982). Total Carbon, Organic Carbon and Organic Matter. In A. L.
799 Page, R. H. Miller, & D. R. Keeney (Eds.), *Methods of soil analysis Part 2 Agronomy 9* (2nd
800 ed., pp. 539–579). American Society of Agronomy.

Neuwald, I. J., Hübner, D., Wiegand, H. L., Valkov, V., Borchers, U., Nödler, K., Scheurer, M., Hale, S. E., Arp, H. P. H., & Zahn, D. (2022). Occurrence, Distribution, and Environmental Behavior of Persistent, Mobile, and Toxic (PMT) and Very Persistent and Very Mobile (vPvM) Substances in the Sources of German Drinking Water. *Environmental Science & Technology*, *56*(15), 10857–10867. https://doi.org/10.1021/acs.est.2c03659

Obia, A., Mulder, J., Martinsen, V., Cornelissen, G., & Børresen, T. (2016). In situ effects of biochar on aggregation, water retention and porosity in light-textured tropical soils. *Soil and Tillage Research*, *155*, 35–44. https://doi.org/10.1016/j.still.2015.08.002

O'Connor, J., Mickan, B. S., Siddique, K. H. M., Rinklebe, J., Kirkham, M. B., & Bolan, N. S. (2022). Physical, chemical, and microbial contaminants in food waste management for soil application: A review. *Environmental Pollution*, *300*, 118860. https://doi.org/10.1016/j.envpol.2022.118860

O'Hagan, D. (2008). Understanding organofluorine chemistry. An introduction to the C–F bond. *Chemical Society Reviews*, *37*(2), 308–319. https://doi.org/10.1039/B711844A

Papari, S., & Hawboldt, K. (2018). A review on condensing system for biomass pyrolysis process. *Fuel Processing Technology*, *180*, 1–13. https://doi.org/10.1016/j.fuproc.2018.08.001

Pennise, D. M., Smith, K. R., Kithinji, J. P., Rezende, M. E., Raad, T. J., Zhang, J., & Fan, C. (2001). Emissions of greenhouse gases and other airborne pollutants from charcoal making in Kenya and Brazil. *Journal of Geophysical Research: Atmospheres*, *106*(D20), 24143–24155. https://doi.org/10.1029/2000JD000041

Raposo, F., & Barceló, D. (2021). Challenges and strategies of matrix effects using chromatography-mass spectrometry: An overview from research versus regulatory viewpoints. *TrAC Trends in Analytical Chemistry*, *134*, 116068. https://doi.org/10.1016/j.trac.2020.116068

Rodgers, K. M., Swartz, C. H., Occhialini, J., Bassignani, P., McCurdy, M., & Schaider, L. A. (2022). How Well Do Product Labels Indicate the Presence of PFAS in Consumer Items Used by Children

826 and Adolescents? *Environmental Science & Technology*, *56*(10), 6294–6304.
827 https://doi.org/10.1021/acs.est.1c05175
828 Schmidt, H.-P., Anca-Couce, A., Hagemann, N., Werner, C., Gerten, D., Lucht, W., & Kammann, C.
829 (2019). Pyrogenic carbon capture and storage. *GCB Bioenergy*, *11*(4), 573–591.
830 https://doi.org/10.1111/gcbb.12553
831 Semerád, J., Hatasová, N., Grasserová, A., Černá, T., Filipová, A., Hanč, A., Innemanová, P.,
832 Pivokonský, M., & Cajthaml, T. (2020). Screening for 32 per- and polyfluoroalkyl substances
833 (PFAS) including GenX in sludges from 43 WWTPs located in the Czech Republic—Evaluation
834 of potential accumulation in vegetables after application of biosolids. *Chemosphere*, *261*,
835 128018. https://doi.org/10.1016/j.chemosphere.2020.128018
836 Sepulvado, J. G., Blaine, A. C., Hundal, L. S., & Higgins, C. P. (2011). Occurrence and Fate of
837 Perfluorochemicals in Soil Following the Land Application of Municipal Biosolids.
838 *Environmental Science & Technology*, *45*(19), 8106–8112.
839 https://doi.org/10.1021/es103903d
840 Sørmo, E., Silvani, L., Thune, G., Gerber, H., Schmidt, H. P., Smebye, A. B., & Cornelissen, G. (2020).
841 Waste timber pyrolysis in a medium-scale unit: Emission budgets and biochar quality.
842 *Science of The Total Environment*, *718*, 137335.
843 https://doi.org/10.1016/j.scitotenv.2020.137335
844 Sparrevik, M., Adam, C., Martinsen, V., Jubaedah, & Cornelissen, G. (2015). Emissions of gases and
845 particles from charcoal/biochar production in rural areas using medium-sized traditional and
846 improved “retort” kilns. *Biomass and Bioenergy*, *72*, 65–73.
847 https://doi.org/10.1016/j.biombioe.2014.11.016
848 Stoiber, T., Evans, S., & Naidenko, O. V. (2020). Disposal of products and materials containing per-
849 and polyfluoroalkyl substances (PFAS): A cyclical problem. *Chemosphere*, *260*, 127659.
850 https://doi.org/10.1016/j.chemosphere.2020.127659

Sunderland, E. M., Hu, X. C., Dassuncao, C., Tokranov, A. K., Wagner, C. C., & Allen, J. G. (2019). A review of the pathways of human exposure to poly- and perfluoroalkyl substances (PFASs) and present understanding of health effects. *Journal of Exposure Science & Environmental Epidemiology*, *29*(2), 131–147. https://doi.org/10.1038/s41370-018-0094-1

Tansel, B. (2022). PFAS use in electronic products and exposure risks during handling and processing of e-waste: A review. *Journal of Environmental Management*, *316*, 115291. https://doi.org/10.1016/j.jenvman.2022.115291

Thoma, E. D., Wright, R. S., George, I., Krause, M., Presezzi, D., Villa, V., Preston, W., Deshmukh, P., Kauppi, P., & Zemek, P. G. (2022). Pyrolysis processing of PFAS-impacted biosolids, a pilot study. *Journal of the Air & Waste Management Association*, *72*(4), 309–318. https://doi.org/10.1080/10962247.2021.2009935

Trimmel, S., Vike-Jonas, K., Gonzalez, S. V., Ciesielski, T. M., Lindstrøm, U., Jenssen, B. M., & Asimakopoulos, A. G. (2021). Rapid Determination of Per- and Polyfluoroalkyl Substances (PFAS) in Harbour Porpoise Liver Tissue by HybridSPE®–UPLC®–MS/MS. *Toxics*, *9*(8). https://doi.org/10.3390/toxics9080183

UNEP. (2017). *Report of the Persistent Organic Pollutants Review Committee on the work of its thirteenth meeting*.

UNEP. (2019). *Perfluorooctane sulfonic acid, its salts and perfluorooctane sulfonyl fluoride* (SC-9/4).

Venkatesan, A. K., & Halden, R. U. (2013). National inventory of perfluoroalkyl substances in archived U.S. biosolids from the 2001 EPA National Sewage Sludge Survey. *Journal of Hazardous Materials*, *252–253*, 413–418. https://doi.org/10.1016/j.jhazmat.2013.03.016

Wang, Z., Cousins, I. T., Scheringer, M., Buck, R. C., & Hungerbühler, K. (2014). Global emission inventories for C4–C14 perfluoroalkyl carboxylic acid (PFCA) homologues from 1951 to 2030, part II: The remaining pieces of the puzzle. *Environment International*, *69*, 166–176. https://doi.org/10.1016/j.envint.2014.04.006

876 Xiao, F., Sasi, P. C., Yao, B., Kubátová, A., Golovko, S. A., Golovko, M. Y., & Soli, D. (2020). Thermal
877 Stability and Decomposition of Perfluoroalkyl Substances on Spent Granular Activated
878 Carbon. *Environmental Science & Technology Letters*, *7*(5), 343–350.
879 https://doi.org/10.1021/acs.estlett.0c00114
880 Xiao, X., Chen, B., Chen, Z., Zhu, L., & Schnoor, J. L. (2018). Insight into Multiple and Multilevel
881 Structures of Biochars and Their Potential Environmental Applications: A Critical Review.
882 *Environmental Science & Technology*, *52*(9), 5027–5047.
883 https://doi.org/10.1021/acs.est.7b06487
884 Yan, H., Zhang, C.-J., Zhou, Q., Chen, L., & Meng, X.-Z. (2012). Short- and long-chain perfluorinated
885 acids in sewage sludge from Shanghai, China. *Chemosphere*, *88*(11), 1300–1305.
886 https://doi.org/10.1016/j.chemosphere.2012.03.105
887 Yao, B., Sun, R., Alinezhad, A., Kubátová, A., Simcik, M. F., Guan, X., & Xiao, F. (2022). V. *Journal of*
888 *Hazardous Materials*, *436*, 129313. https://doi.org/10.1016/j.jhazmat.2022.129313
889 Ye, L., Peng, Z., Wang, L., Anzulevich, A., Bychkov, I., Kalganov, D., Tang, H., Rao, M., Li, G., & Jiang, T.
890 (2019). Use of Biochar for Sustainable Ferrous Metallurgy. *JOM*, *71*(11), 3931–3940.
891 https://doi.org/10.1007/s11837-019-03766-4
892 Zafeiraki, E., Costopoulou, D., Vassiliadou, I., Bakeas, E., & Leondiadis, L. (2014). Determination of
893 perfluorinated compounds (PFCs) in various foodstuff packaging materials used in the Greek
894 market. *Chemosphere*, *94*, 169–176. https://doi.org/10.1016/j.chemosphere.2013.09.092
895 Zhang, J., Smith, K. R., Ma, Y., Ye, S., Jiang, F., Qi, W., Liu, P., Khalil, M. A. K., Rasmussen, R. A., &
896 Thorneloe, S. A. (2000). Greenhouse gases and other airborne pollutants from household
897 stoves in China: A database for emission factors. *Atmospheric Environment*, *34*(26), 4537–
898 4549. https://doi.org/10.1016/S1352-2310(99)00450-1
899 Zhang, W., Pang, S., Lin, Z., Mishra, S., Bhatt, P., & Chen, S. (2021). Biotransformation of
900 perfluoroalkyl acid precursors from various environmental systems: Advances and

perspectives. *Environmental Pollution*, *272*, 115908.
https://doi.org/10.1016/j.envpol.2020.115908